CaMKII binds both substrates and effectors at the active site

Can Özden[1,2], Roman Sloutsky[1], Nicholas Santos[1], Emily Agnello[1], Christl Gaubitz[4], Emily Lapinskas[1], Edward A. Esposito[3], Brian A. Kelch[4], Scott C. Garman[1], Yasunori Hayashi[5], Margaret M. Stratton[1]†

[1]Department of Biochemistry and Molecular Biology, University of Massachusetts, Amherst, MA 01003, USA. [2]Molecular and Cellular Biology Graduate Program, University of Massachusetts, Amherst, MA 01003, USA. [3]Malvern Panalytical, [4]Department of Biochemistry and Molecular Pharmacology, University of Massachusetts, Worcester, MA 01605, USA. [5]Department of Pharmacology, Kyoto University Graduate School of Medicine, Kyoto, Japan.

† Corresponding author. Email: mstratton@umass.edu (M.M.S.)

ABSTRACT

Ca^{2+}/calmodulin dependent protein kinase II (CaMKII) is a signaling protein that is required for successful long-term memory formation. Ca^{2+}/CaM activates CaMKII by binding to its regulatory segment, thereby making the substrate binding pocket available. One exceptional feature of this kinase is that two binding partners have been shown persistently activate CaMKII after the Ca^{2+} stimulus dissipates. The molecular details of this phenomenon are unclear. Despite having a large variety of interaction partners, the specificity of CaMKII has not been structurally well-characterized. To this end, we solved X-ray crystal structures of the CaMKII kinase domain bound to four different binding partners: a peptide substrate, a substrate/activator, a substrate/binding partner, and an inhibitor (AMPA-type glutamate receptor, NMDA-type glutamate receptor, Tiam1, and Densin-180). We show that all four binding partners use similar interactions to bind across the substrate binding pocket of the CaMKII active site. We generated a sequence alignment based on our structural observations, which revealed conserved interactions across these binding partners. The structures presented here shed much-needed light on the interaction between CaMKII and its binding partners. These observations will be crucial in guiding further biological experiments.

INTRODUCTION

Ca^{2+}/calmodulin-dependent protein kinase II (CaMKII) is a central signaling protein that controls various cellular functions such as synaptic plasticity, cytoskeletal regulation, cell growth and division, gene transcription and ion channel modulation [1]. CaMKII biology has been an active focus of research especially because of its crucial role in long-term potentiation (LTP), which is the basis for long-term memory [2, 3]. CaMKII is a highly abundant in the forebrain postsynaptic density (PSD) fraction, where it makes up to 2% of total protein [4]. CaMKII is a multisubunit complex made up of 12-14 subunits, which is oligomerized by the hub domain (**Fig. 1A**). Each CaMKII subunit contains a Ser/Thr kinase domain, autoinhibitory/regulatory segment, variable linker region, and a hub domain (**Fig. 1B**).

CaMKII interacts with and phosphorylates dozens of synaptic proteins also known to play key roles in LTP (**Fig. 1C**). Intriguingly, some binding partners are substates, some are inhibitors, and some have been shown to persistently activate CaMKII. The structural details explaining these disparities remain elusive. To begin untangling this, we first need to understand the specificity driving these interactions. We chose to structurally characterize four peptides from interactors that sample multiple functional outputs: AMPA-type glutamate receptor is a substrate, NMDA-

type glutamate receptor is a substrate and activator, Tiam1 is an activator, and Densin-180 is an inhibitor.

Ca^{2+}/calmodulin (Ca^{2+}/CaM) activates CaMKII by binding to the regulatory segment and thereby freeing the substrate binding pocket. This well-understood mechanism triggers autophosphorylation of T286 within the autoinhibitory segment, which renders CaMKII constitutively active. CaMKII is also activated by another mechanism, for which we lack a clear mechanism. There are two binding partners (NMDA receptor and Tiam1) that have been shown to be activators of CaMKII after the Ca^{2+} stimulus dissipates [5-7]. The GluN2B subunit of the NMDA receptor is a known substrate of CaMKII, and to this point, the best studied CaMKII activator. Ca^{2+}/CaM-activated CaMKII has been shown to form a persistent complex with GluN2B, which locks CaMKII in an active conformation, as long as binding persists. To date, persistent binding of CaMKII to GluN2B and resultant persistent activation has been explained by a hypothetical sequential transition model [7] . In this model, GluN2B first binds to CaMKII close to the active site (termed S-site), presenting Ser 1303 for transphosphorylation. Next, GluN2B changes its position away from the active site and toward the base of CaMKII C-lobe (termed T-site), while freeing S-site to bind other substrates. Although this model has been widely accepted in the field, there has been no structural confirmation.

In addition to structurally interrogating the NR2B interaction, we are additionally studying Tiam1, Densin-180, and AMPA receptor, all of which play key roles in LTP and interact with CaMKII. Tiam1 is a Rac guanine-nucleotide exchange factor (RacGEF), and also a CaMKII substrate. However, the Tiam1 peptide we interrogate here is a known activator, as mentioned above, and a pseudosubstrate (Ala at the phosphorylation site) [6]. Densin-180 (LRRC7) is a postsynaptic scaffolding protein and the peptide we use herein is a known inhibitor of CaMKII (Ile at the phosphorylation site) [8, 9]. Finally, the AMPA receptor subunit GluA1 is a CaMKII substrate but not a known activator. GluA1 phosphorylation has been shown to be important for synaptic plasticity [10-12]. There are two existing crystal structures of the CaMKII kinase domain bound to different effectors. One is CaMKIINtide, a peptide inhibitor of CaMKII derived from CaMKIIN1 [13] and the second is the *Drosophila* EAG potassium channel (*d*EAG) carboxyl tail, which is a known CaMKII substrate [14].

In the current study, we solved four new co-crystal structures of the CaMKII kinase domain bound to peptides from GluN2B, Tiam 1, Densin-180, and GluA1. These structures show the peptides bound in the same binding site on the kinase domain as previously observed with *d*EAG and CaMKIINtide. Combining this structural information has allowed us to clarify important interactions that drive these binding reactions.

RESULTS

CaMKII kinase domain interactions with four different binding partners

We used a fluorescence polarization (FP) assay to measure binding of CaMKII kinase domain to peptides of five interactors: GluN2B (1289-1310), GluA1 (818-837), Densin-180 (797-818), Tiam1 (1541-1559), and CaMKIINtide (37-58). Four out of five tested peptides bind with similar affinities (K_d values 1.3 - 4.5 μM) (GluN2B K_d = 1.3 μM, CaMKIINtide K_d = 2.9 μM, Densin-180 K_d = 3.4 μM, and Tiam1 K_d = 4.5 μM) (**Fig. 2B**). The one exception was GluA1, which bound with a significantly lower affinity compared to the others (K_d = 95 μM) (**Fig. 2B**). For comparison, we include CaMKIINtide in these studies, as this is a known endogenous inhibitor of CaMKII [15-17]. Unless otherwise specified, crystallographic and fluorescence polarization (FP) experiments were conducted in the background of an inactivating CaMKII mutation (D135N). Herein, we will highlight key interactions observed in the structures that mediate these interactions.

We solved crystal structures of the kinase domain of CaMKII bound to four peptides of known interactors (**Fig. 2**). These include NMDA and AMPA receptor peptide substrates (GluN2B 1289-1310 and GluA1 818-837, respectively), Densin-180 (797-818) and Tiam1 (1541-1559). All four crystal structures have resolutions within the range of 1.8 - 2.7 Å (Table 1). The overall fold of the kinase domain is similar in all structures with a range of Cα RMSD values from 0.583 to 1.611 Å.

We solved 6 structures of the CaMKII kinase domain bound to GluN2B peptide variants with different molecules bound in the active site. In two structures, the D135N kinase domain is bound to the GluN2B peptide with either ATP (PDB:6XBX) or methyl 6-O-(N-heptylcarbamoyl)-alpha-D-glucopyranoside (Hecameg), a mild detergent molecule, in the active site. Both ATP and Hecameg form hydrogen bonds with the backbone carboxy group of D90 and the backbone amino group of V92. We then solved structures of the D135N kinase domain bound to a phosphomimetic version of the GluN2B peptide (S1303D), with both ATP and HECAMEG bound. Finally, WT kinase domain was crystallized with the GluN2B peptide bound with either ADP bound (PDB:6XDU) or an empty active site (PDB:6XDL). In these structures, there was better resolution at the C-terminus of the peptide compared to previous structures.

All peptides bound similarly, interacting with a similar surface on the kinase domain. We resolved 14-19 residues in each peptide (**Fig. 2A, S1**). GluN2B and Densin-180 bound in a completely extended conformation across the substrate binding pocket, whereas Tiam1 and GluA1 adopt short helical turns at the N-terminal end of the peptides, similar to what was previously observed in the CaMKIINtide structure [13]. Additionally, Densin-180 forms an intrachain electrostatic interaction between the -3 position arginine and upstream aspartate.

Sequence alignment of CaMKII binding partners based on high-resolution structures

So far, prediction of CaMKII interaction partners has been difficult due to conformational heterogeneity in CaMKII binding. Our structures reveal several peptides have helical turns that shift the register of conserved interactions (Tiam1, GluA1, and the previously observed CaMKIINtide). We now provide updated sequence alignments based on our structural observations (**Fig. 2C**). The two peptides that are substrate (GluN2B and GluA1) have the phosphosite (highlighted purple in Fig. 2C) facing the ATP binding pocket, such that both peptides are docked at the active site, ready to be phosphorylated. The critical residues of the binding partner involved in mediating this interaction are conserved at positions +1, -2, -3, -5, and -8 (**Fig. 2C**). Herein, we use numbering based on the prototypical GluN2B substrate with the phosphorylation site set to zero, irrespective of actual number of in each protein.

Our structures are consistent with the previous data suggesting that substrate positions +1, -2 and -3 are important for binding. It had been noted that a small hydrophobic residue is preferred at the +1 position [14, 18-21], which we also observe in our structures. Val and Ile at the +1 position bind to the hydrophobic groove across G175 (see **Fig. S5**), whereas Tyr of GluN2B was too large to fit into this groove and therefore points away. Glutamine is commonly noted at the -2 position [14, 18-20], however it was previously unclear why this is favored due to insufficient structural data. All four of the peptides used in this study contain glutamine at this position, allowing us to resolve important interactions mediated at this position. We observe the amide oxygen of the glutamine sidechain forms a hydrogen bond with the backbone of G178, and the amino group interacts with the sidechain of Y179 of CaMKII. Additionally, the backbone carbonyl of glutamine interacts with sidechain of K137, and the backbone amino group of the -2 position interacts with E139, which has also been shown to be important for binding (**Fig. S3**) [7]. Of note, CaMKIINtide has a serine residue at the -2 position instead of glutamine. In this structure, the serine sidechain is flipped relative to the glutamine sidechains, which enables hydrogen bonding with E139 and K137 sidechains [13]. This observation is consistent with a previous study, which

showed that CaMKIINtide binding to CaMKII was reduced when this serine was mutated to alanine [22]. Finally, the -3 position is conserved to be a basic residue, which interacts with conserved glutamate residues on the kinase domain (E96, E99), similar to previous observation [13, 23]. This interaction is discussed further below.

Hydrophobic residues mediate all observed binding interactions

Hydrophobic interaction mediated by a conserved leucine. All CaMKII interactors use a conserved leucine residue at the -5 position to bind in a conserved leucine at the -5 position interacts with a hydrophobic pocket on the kinase domain comprised of F98, I101, V102, and I205 (**Fig. 3A, S5**). The leucine residue is 3.3-4.5 Å away from the four hydrophobic residues, indicating tight interactions. In the CaMKIINtide structure, a turn motif is facilitated by two glycine residues, which orients the leucine into this pocket.

Docking site mediated by W214. Both Densin-180 and CaMKIINtide pack against a tryptophan residue on the kinase domain (W214) (**Fig. 3B**). In both structures, the sidechains of proline and isoleucine (highlighted green in **Fig. 2C**) pack against this tryptophan. Additionally for Densin-180, the guanidino group of R808 at the -7 position hydrogen bonds with the carbonyl group of W214 and the sidechain of Q224. Using our FP assay, we measured substrate binding to a kinase domain mutant (W214A) to determine the role of this tryptophan in docking. The W214A mutation completely abolished CaMKIINtide binding, whereas the effects on Densin-180, NR2B, GluA1, and Tiam1 binding were not as severe, decreasing the binding affinity 2- to 3-fold (**Fig. 3C, S2**).

Electrostatic interactions may provide specificity

Conserved salt bridge close to the active site. All interactors except for low-affinity binder GluA1 use a conserved basic residue at the -3 position to form salt bridge with two glutamic acid residues (E96, E99) located on the αD helix of the kinase domain (Fig. 4A). These basic residues of interaction partners are positioned 2.4 - 4.2 Å between the E96 and E99. In the Densin-180 and CaMKIINtide structures, the -3 residue is closer to E96, whereas in the Tiam1 structure, the -3 position is closer to E99. In the structures of GluN2B, the -3 position is either more closely associated with E96 (PDB:6XDL, WT kinase with empty active site; PDB:6XDU, WT kinase with ADP bound) or E99 (PDB:6XBP, D135N kinase with a detergent bound; PDB:6XBX, D135N kinase with ATP bound). Additionally, in structures where ATP/$MgCl_2$ is also bound (GluN2B, Tiam1), the side chain of E96 interacts with the hydroxyl group of ribose in the ATP molecule ((3.7 – 4.3 Å; **Fig. S4**) [24]. This salt bridge is not formed in the GluA1 interaction, because there is a proline at the -3 position. In the GluA1 co-crystal structure, the sidechain of E96 is flipped away from the substrate compared to the other four structures where it is oriented toward the binding partner (**Fig. 4A**, inset). Additionally, the sidechain of E99 is not as well-resolved as it is in the other structures.

We hypothesized that the reason for GluA1's lower affinity compared to other interaction partners is due to the lack of this salt bridge. To test this, we created charge reversal mutations (E→K) and also E→Q mutations to maintain hydrogen bonding but not the electrostatic component. We directly compared binding affinities of GluN2B (which has a basic residue at the -3 position) to GluA1 which is lacking this interaction. Single E99K and E96K mutations were more disruptive to GluN2B binding (affinity decreased 5- and 7-fold, respectively) compared to GluA1 binding (affinity decreased <2-fold) (**Fig. 4B, C**). The double lysine mutation (E96/99K) significantly reduced the binding affinity for GluN2B peptide 52-fold (K_d = 68.7 μM), while the affinity for GluA1 was roughly the same.

Overall, the E→Q mutations were less disruptive to binding. GluN2B binding to E96Q and E99Q was only marginally impaired (affinity decreased <2-fold), while the binding affinity of GluN2B for the double mutant E96/99Q was weakened by ~4-fold (K_d = 5 μM) (**Fig. S3B**). All glutamine mutants showed similar binding to GluA1 compared to WT, where the binding affinities were >77 μM (**Fig. S3C**). The double glutamine mutant (E96/99Q) expressed more poorly than WT, but the double lysine mutant (E96/99K) reduced the protein expression significantly likely due to destabilization.

Salt bridge at the base of the C-lobe. We observed a previously uncharacterized conserved basic residue at the -8 position (arginine or lysine) mediating a salt bridge with E236 on the kinase domain (**Fig. 5A, S5**). This likely has not been previously characterized likely because this position is quite far (~30 Å) from the phosphorylation site, and substrate alignments have not been accurate enough to highlight this position.

We tested the effect of mutating E236 to lysine (E236K) on binding affinity. The E236K mutation completely abolished both Tiam1 and CaMKIINtide binding, whereas the effects on GluN2B, Densin-180, and GluA1 binding were more subtle (**Fig 5B, S7**). For Densin-180, E236K binding affinity was reduced ~6-fold (K_d = 21 μM). Consistent with previous studies, the E236K mutation did not entirely disrupt the interaction with the GluN2B peptide [7], but the K_d was weakened ~7-fold (K_d = 9 μM). We investigated whether peptide phosphorylation would have an effect on binding affinity, so we measured the affinity of D135N and D135N/E236K to the GluN2B peptide with a phosphomimetic substitution (S→D at position 0). There was very little effect on binding to D135N (K_d = 2 μM), whereas the affinity for and D135N/E236K was reduced 20-fold to 44 μM (**Fig. 5C**).

DISCUSSION

CaMKII has a broad range of substrates and interaction partners, yet the interaction surface has not been structurally characterized. We addressed this by solving co-crystal structures of four binding partners bound to the CaMKII kinase domain, which allowed us to highlight the interactions mediating binding. Like many other kinases, CaMKII was predicted to have an electrostatic interaction with a basic residue at the -3 position [25]. E96 is well-conserved across kinases and known to be important for ATP binding (**Fig. 5D**) [24]. E99 is not as well-conserved, even across other CaM-kinases (**Fig. 5D**) [26]. Our mutagenesis data suggest that the decreased affinity of GluA1 to CaMKII is largely due to the absence of this salt bridge because charge reversal mutations do not significantly affect the affinity. The biological ramifications of this weak interaction between CaMKII and GluA1 will need to be investigated – where localization of CaMKII to this receptor by another factor or avidity effects of holoenzyme localization [27] may be driving GluA1 phosphorylation.

All kinases adopt conformational changes upon activation. In CaMKII activation, the αD helix reorients outward, exposing a hydrophobic pocket for substrate binding, which we observed in all our structures. Kuriyan and colleagues first identified this hydrophobic pocket as 'docking site B', which is comprised of residues F98, I101, V102, and I205 [13]. Highlighting the importance of this hydrophobic interaction, an F98 mutation has been shown to cause intellectual disability [28]. This hydrophobic pocket is highly conserved across CaM-kinases, whereas these hydrophobic residues are no longer conserved once the alignment is expanded to include other kinases (**Fig. 5D**). If we compare the structure of the kinase domain with an empty substrate binding site (PDB:6VZK) to structures of the kinase domain bound to a substrate, it is clear that F98 and V102 undergo a conformational change in the bound state to form a pocket (**Fig. S6A**). This indicates that these hydrophobic residues shift to accommodate substrate binding, which is likely a large

contribution to an observed gain in stability upon NR2B binding (**Fig. S6B**), similar to what we have previously observed with regulatory segment binding [29].

In the autoinhibited state, this hydrophobic binding pocket is protected from solvent by regulatory segment binding (mediated by L290) [29]. This interaction with the regulatory segment is very similar to all interaction partners we crystallized, despite the fact that regulatory segment adopts a completely helical conformation. The phenylalanine (F98) and isoleucine (I205) of this hydrophobic pocket have been reported as potentially playing different roles in binding interactions, previously termed S- and T-sites, respectively [7, 23]. However, our data show that these residues comprise the same binding pocket. Our binding data did not reveal any heterogeneity in binding. Further structural and biophysical analyses will necessary to elucidate how some binding proteins, including GluN2B and Tiam1, can act as CaMKII activators while masking the entire substrate binding pocket (both S- and T-sites). For these experiments it will be important to consider the holoenzyme structure and how interacting with different downstream partners may affect adjacent kinases within a complex.

CaMKIINtide and the peptide of Densin-180 used here are both inhibitors of CaMKII and these structures revealed a novel interaction mediated by W214 on the kinase domain. Surprisingly, mutating this residue in the kinase to alanine (W214A) abolished CaMKIINtide binding completely while only having a marginal effect on Densin-180. Upon close examination, CaMKIINtide docking onto W214 stabilizes its helical motif, which orients the -5 position leucine into the hydrophobic pocket. When W214 is mutated, this interaction is disrupted and leucine interaction is unlikely to be maintained, completely disrupting binding. These data suggest that W214 can serve as a docking site for some CaMKII interaction partners, but not all. A role for W214 was also proposed as a result of molecular dynamics simulation with Coenzyme A [30].

In all our structures, a conserved basic residue at the N-terminal end of the binding partners forms a salt bridge with E236 on the kinase domain. In the crystal structure solved with the kinase domain bound to a *d*EAG peptide, there is a glutamine residue interacting with E236 [14]. The effect of mutation at this site (E236K) had previously been tested on GluN2B binding, which did not show a significant change [7]. In our measurements, there was consistently a decrease in affinity of peptides binding to E236K, but to different degrees. More work needs to be done to determine whether this electrostatic interaction provides some specificity, which could be exploited in biological experiments.

Finally, we mined the curated database of CaMKII phosphorylation sites (n=418) for consistencies with our updated alignment and found that the substrate recognition by CaMKII in our crystal structures can be further generalized (**Fig. 5E**, www.phosphosite.org). Hydrophobic residues (I, V, L, M, F) are found in +1, Q is found at -2, R is found at -3 but also at -2 and -4. L, I or M is found at -5 but also in -6. Generally, the upstream sequence disfavors P, D, and E, suggesting that a conformation ridigity and negative charge are not favored. In contrast, D at +2 is favored. We observe in our GluN2B-bound structures that D at +2 is in close proximity with K56, such an interaction was observed previously in *d*EAG-bound structure (PDB: 5H9B), which is likely to drive the preference for D at this position. In addition, S, which may serve as a second phosphorylation site, is also disfavored in both upstream and downstream [14].

There is mounting evidence that specific interactions lead to either persistent CaMKII activity or inhibition, yet there is not a molecular explanation for this. Based on our structures and mutagenesis, it seems clear that certain interactions dominate the binding energy in some binding partners but not others, giving us an indication of specificity. As previously mentioned, to fully understand effector binding to CaMKII, future work will need to visualize these interactions in the

context of the holoenzyme. The crystal structures presented here provide clarity on the specific interactions between CaMKII and its binding partners, which will be crucial in biological experiments to assess the downstream effects of specific interactions. These observations will be crucial in guiding further experiments, which will necessarily invoke the complexities of the CaMKII holoenzyme structure.

METHODS

Cloning

All CaMKIIα variants were expressed with an N-terminal His-SUMO tag in a pET vector. All point mutations were created using site-directed mutagenesis.

Protein Expression and Purification

WT CaMKIIα kinase domain (residues 7-274) was co-expressed with λ phosphatase in *E. coli* BL21(DE3). Inactive constructs (D135N) were expressed without λ phosphatase. The cells were induced at 18 °C with 1 mM Isopropyl β- d-1-thiogalactopyranoside (IPTG) and grown overnight. Following to ~16 hours incubation, cell pellets were resuspended in Buffer A (25 mM Tris, pH 8.5, 150 mM KCl, 40 mM imidazole, 10% glycerol) and commercially available protease inhibitors (0.5 mM Benzamidine, 0.2 mM AEBSF, 0.1 mg/mL trypsin inhibitor, 0.005 mM Leupeptin, 1 µg/mL Pepstatin), 1 µg/mL DNAse/50 mM $MgCl_2$ were added, then lysed. All following purification steps were performed using an ÄKTA pure chromatography system at 4 °C. Filtered cell lysate was loaded onto a 5 mL His Trap FF NiNTA Sepharose column (GE), and eluted with 50% Buffer B (25 mM Tris-HCl pH 8.5, 150 mM KCl, 1 M imidazole, 10% glycerol). The protein was desalted from excess imidazole using a HiPrep 26/10 Desalting column using Buffer C (25 mM Tris-HCl pH 8.5, 40 mM KCl, 40 mM imidazole, 2 mM TCEP, 10% glycerol). His SUMO tags were cleaved with Ulp1 protease overnight at 4 °C. Cleaved His SUMO tags were separated by a subtractive NiNTA step prior to an anion exchange step. Proteins were eluted from HiTrap Q-FF with a KCl gradient. Eluted proteins were concentrated and further purified in gel filtration buffer (25 mM Tris-HCl pH 8.0, 150 mM KCl, 1 mM TCEP, 10% glycerol) using Superdex 75 10/300 GL size exclusion column. Fractions (>95% purity) were pooled, concentrated, aliquoted and flash frozen in liquid nitrogen, and stored at -80 °C until needed.

Peptide synthesis

Peptides used for co-crystallization were synthesized and amidated at the C-terminus (Genscript, RIKEN Research Resource Center). Peptides used for fluorescence polarization assays were synthesized with an additional N-terminal 5-FAM.

Full length peptide sequences are as follows:
Human GLUA1 (residues 818-837): SKRMKGFCLIPQQSINEAIR [Numbering for GluA1 is for mature peptide, excluding 18 amino acid long signal peptide, following convention in the field.]
Human GluN2B (residues 1289-1310): KAQKKNRNKLRRQHSYDTFVDL
Human GluN2B(S1303D) (residues 1289-1310): KAQKKNRNKLRRQHDYDTFVDL
Human Densin-180 (residues 797-818): SKSRSTSSHGRRPLIRQDRIVG
Mouse Tiam1 (residues 1541-1559): RTLDSHASRMTQLKKQAAL

Full length peptide sequences for fluorescence polarization assays are as follows:
Human GluA1 (residues 813-837): KSRSESKRMKGFCLIPQQSINEAIR
Human GluN2B (residues 1289-1310): KAQKKNRNKLRRQHSYDTFVDL
Human GluN2B(S1303D) (residues 1289-1310): KAQKKNRNKLRRQHDYDTFVDL
Human Densin-180 (797-818): SKSRSTSSHGRRPLIRQDRIVG

Human CaMK2N1 (residues 37-58): GAGQNKRPPKLGQIGRSKRVVI
Mouse Tiam1 (residues 1541-1559): RTLDSHASRMTQLKKQAAL

Crystallization and X-Ray Data Collection
Initial crystallization screening was done by the sitting vapor diffusion method at 4^{o}C using commercially available screening kits. Initial hits were optimized by the hanging vapor diffusion method if needed. Conditions yielded the crystal formation were included in Table S1. The ligand-to-protein ratio was kept at 3:1 throughout the co-crystallization attempts. Diffraction data were collected from crystals flash-frozen in liquid nitrogen at a wavelength of 1.5418 Å using a Rigaku MicroMax-007 HF X-ray source, which was coupled to a Rigaku VariMax HF optic system (UMass Amherst). The X-ray data was collected at 100 K.

Data Processing and Structure Determination
Data sets were integrated, merged, and scaled using HKL-2000. The structures were solved by molecular replacement (MR) with Phaser using the coordinates of CaMKIIα kinase domain (PDB ID: 6VZK, 100% amino acid sequence identity) as a search model. Peptides were built into electron density using Coot and refinement was performed with REFMAC5.

Binding assays
The fluorescent polarization experiment was executed by adding 10 µL of 120 nM fluorescein-labeled peptides (dissolved in 25 mM Tris pH 7.5, 150 mM KCl, 0.02% Tween, 0.02% Triton) to 10 µL of mutant CaMKII kinase domains at varying concentrations (25 mM Tris pH 7.5, 150 mM KCl, 1 mM TCEP, 10% glycerol) in Corning low volume 384-well black flat bottom 384-well plates. The fluorescence polarization was measured using a Synergy H1 hybrid plate reader (Biotek) with a filter of 485/20 nm excitation and 528/20 nm emission. Data were fit using One site- Specific binding with Hill slope in GraphPad PRISM version 6.01 after subtracting the background value from individual values.

ACKNOWLEDGMENTS

We thank Roger Colbran for helpful discussions. This work was supported by start-up funds from UMass Amherst (M.S.), SPIRITS 2019 of Kyoto University, Grant-in-Aid for Scientific Research 18H04733, and 18H05434 from the MEXT, Japan and HFSP Research Grant (RGP0020/2019) (Y.H.).

Conflict of interest: YH received research funds from Fujitsu Laboratories and Dwango.

FIGURES

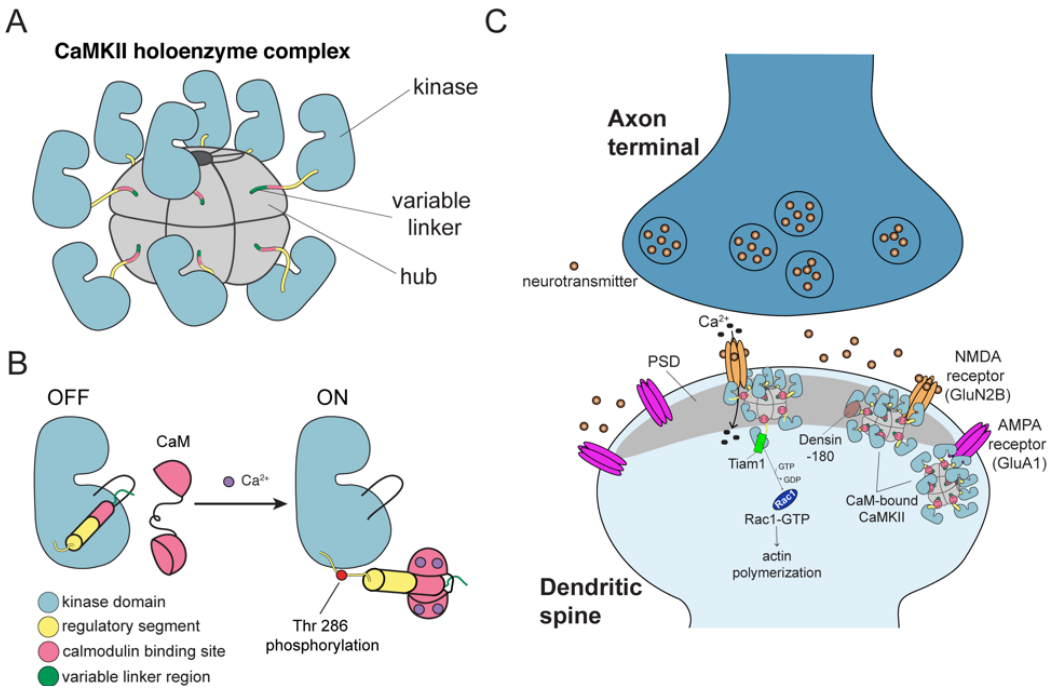

Figure 1. CaMKII architecture and the interaction partners in excitatory synapses (A) The architecture of a dodecameric CaMKII holoenzyme. (B) Ca^{2+}/CaM binding activates CaMKII by competitively binding the regulatory segment thereby freeing the substrate binding pocket. Active CaMKII autophosphorylates at Thr 286. (C) CaMKII interactions at the excitatory postsynaptic structure, mostly in the post synaptic density (PSD).

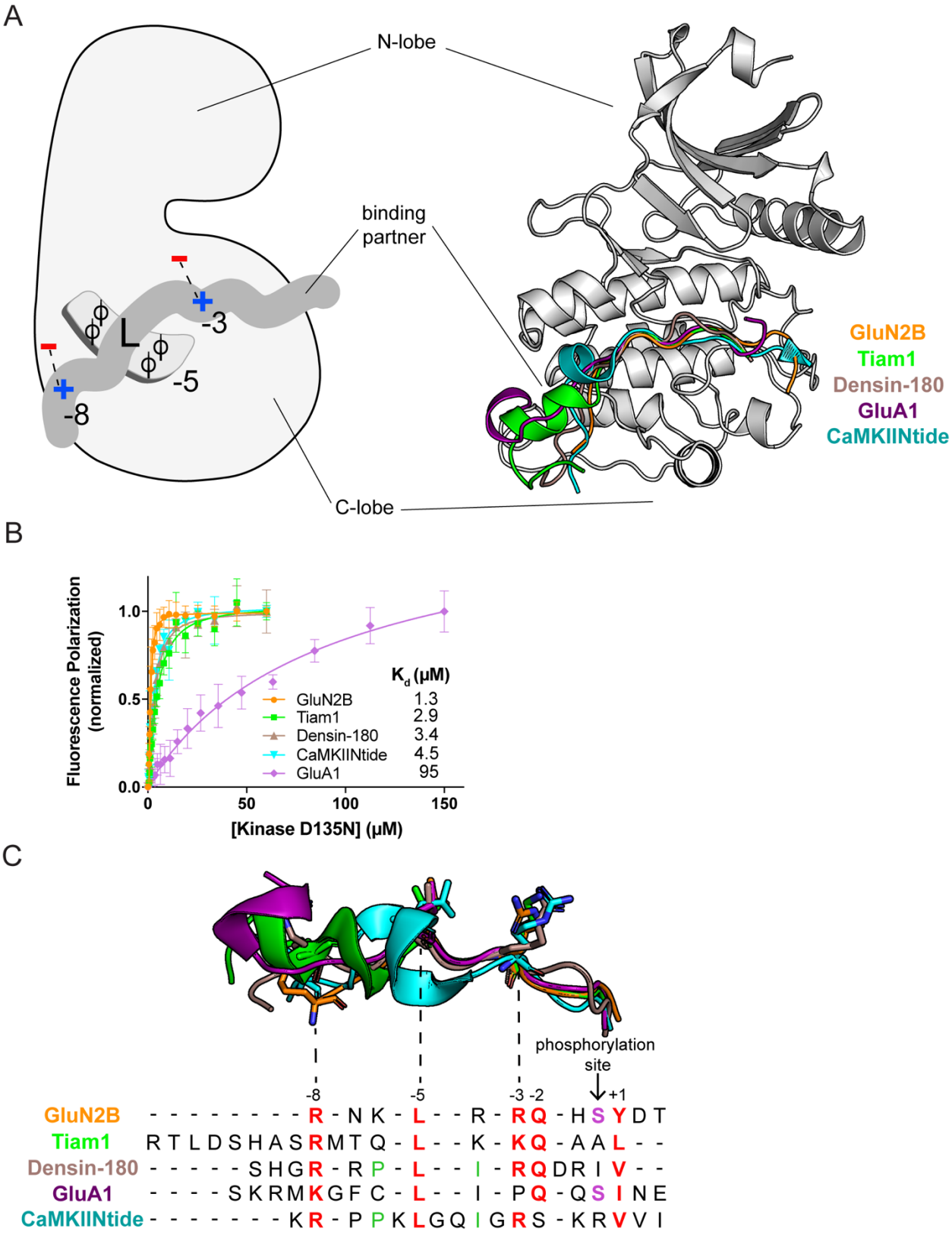

Figure 2. CaMKII kinase domain interactions with the binding partners. (A) (Left) Schematic diagram of the interactions with binding partners. Phi symbol indicates hydrophobic

residues, (right) overlay of five cocrystal structures, peptides shown as cartoon in corresponding colors in (A). (B) Binding measurements for GluN2B, Tiam1, Densin-180, CaMKIINtide, and GluA1 using fluorescence polarization. (C) The sequence alignment of CaMKII binding partners. Aligned peptide structures are above. Conserved residues highlighted in red. Phosphosite residues on substrates highlighted in purple. Residues involved in a docking event with W214 are highlighted in green.

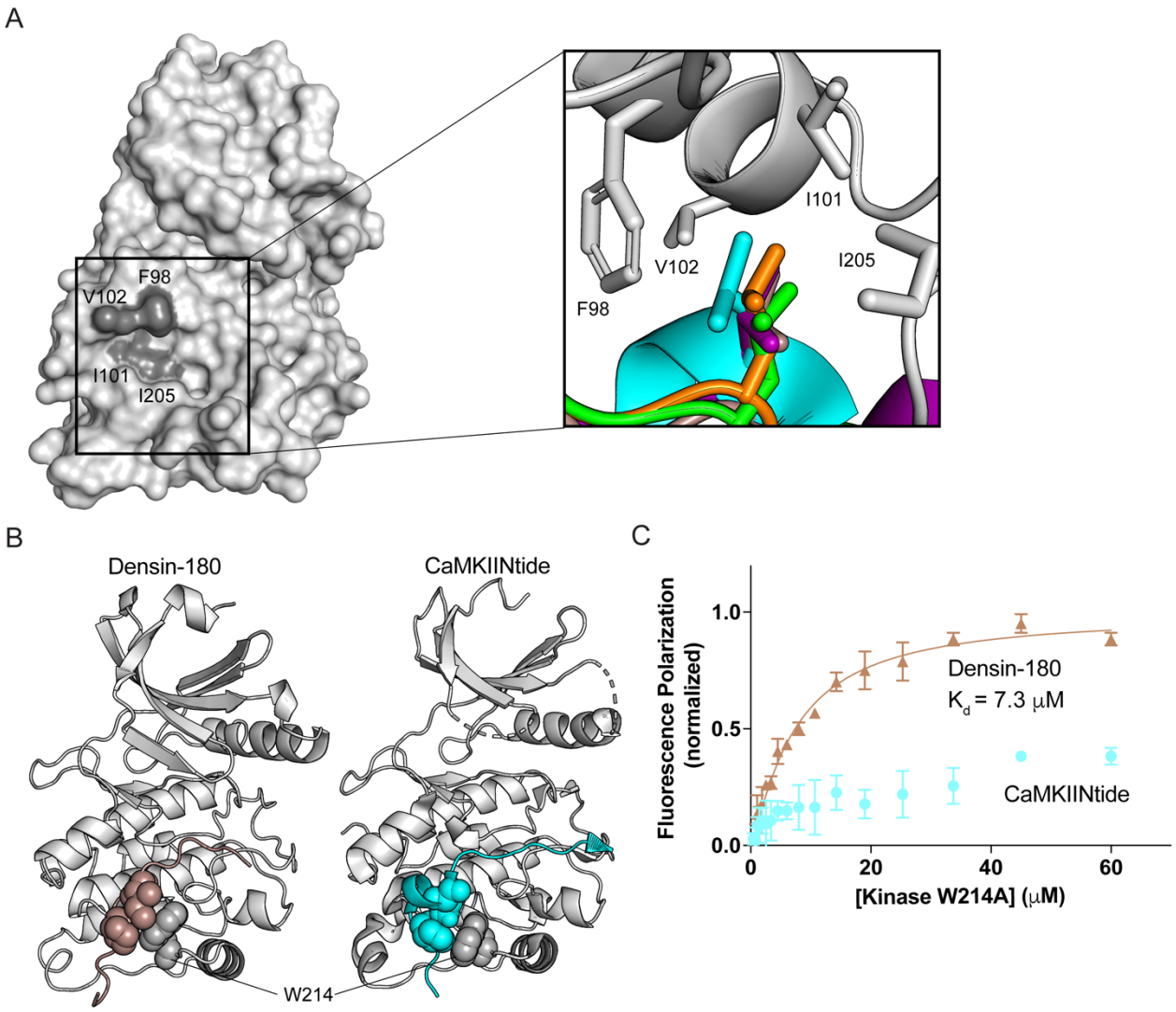

Figure 3. Hydrophobic interactions play mediate binding. (A) Surface representation of CaMKII kinase domain with residues forming the hydrophobic pocket labeled. Zoom in: Overlay of leucine residues from all co-crystal structures bound in the hydrophobic pocket. (B) Sphere representation of the isoleucine and proline residues of Densin-180 (brown) and CaMKIIN (cyan) docking onto W214 (gray) of kinase domain. (C) FP measurements of the CaMKII kinase domain with W214A mutation binding to CaMKIIN (cyan) and Densin-180 (brown) peptides.

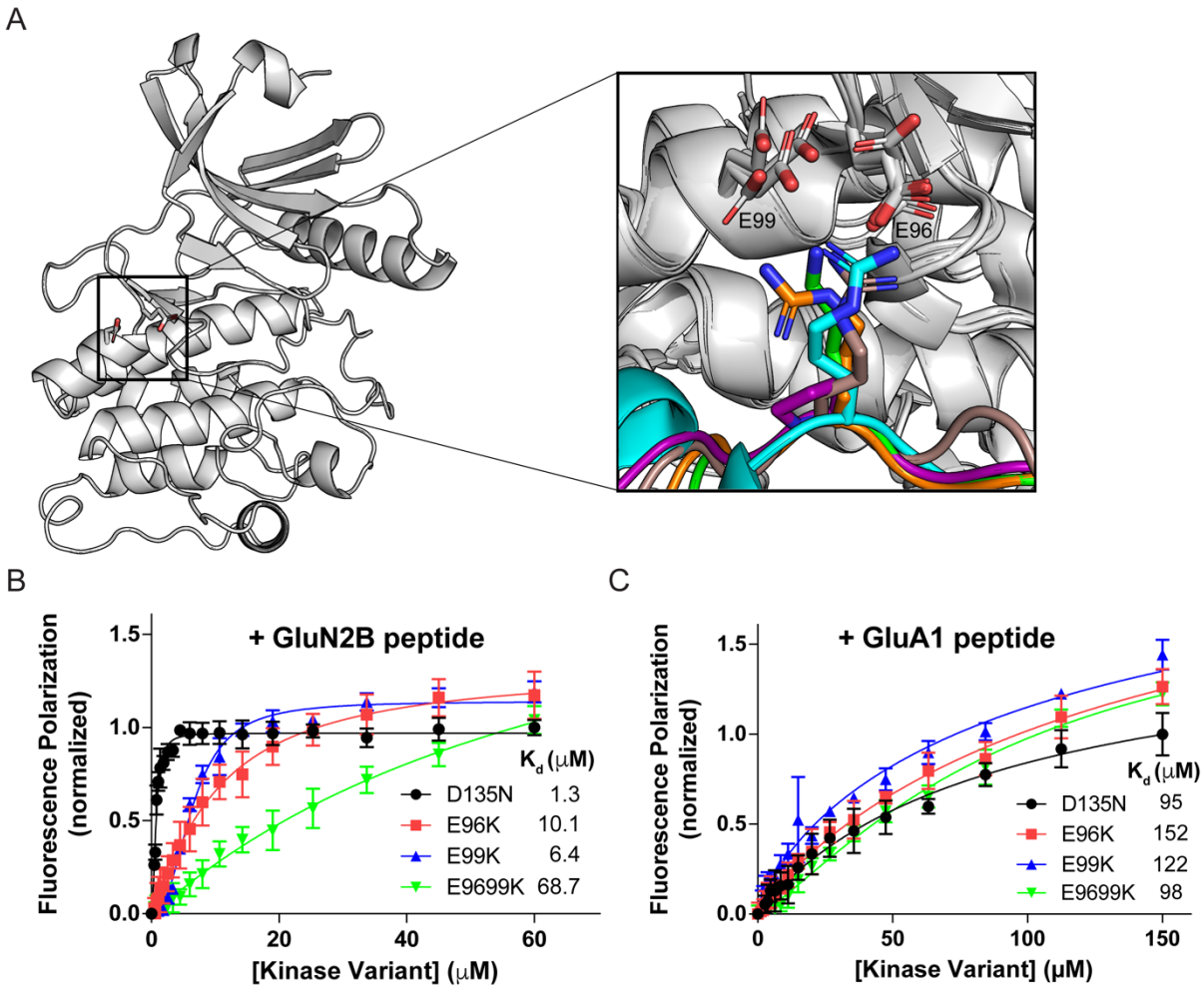

Figure 4. Electrostatic interactions with E96 and E99 facilitate high affinity binding. (A) CaMKII kinase domain shown as a cartoon, E96 and E99 residues are shown in sticks. Inset: zoom in of all five co-crystal structures overlaid. B) FP measurements of the CaMKII kinase domain with E96K (red), E99K (blue), and E9699K (green) mutations binding to the GluN2B peptide and (C) to the GluA1 peptide.

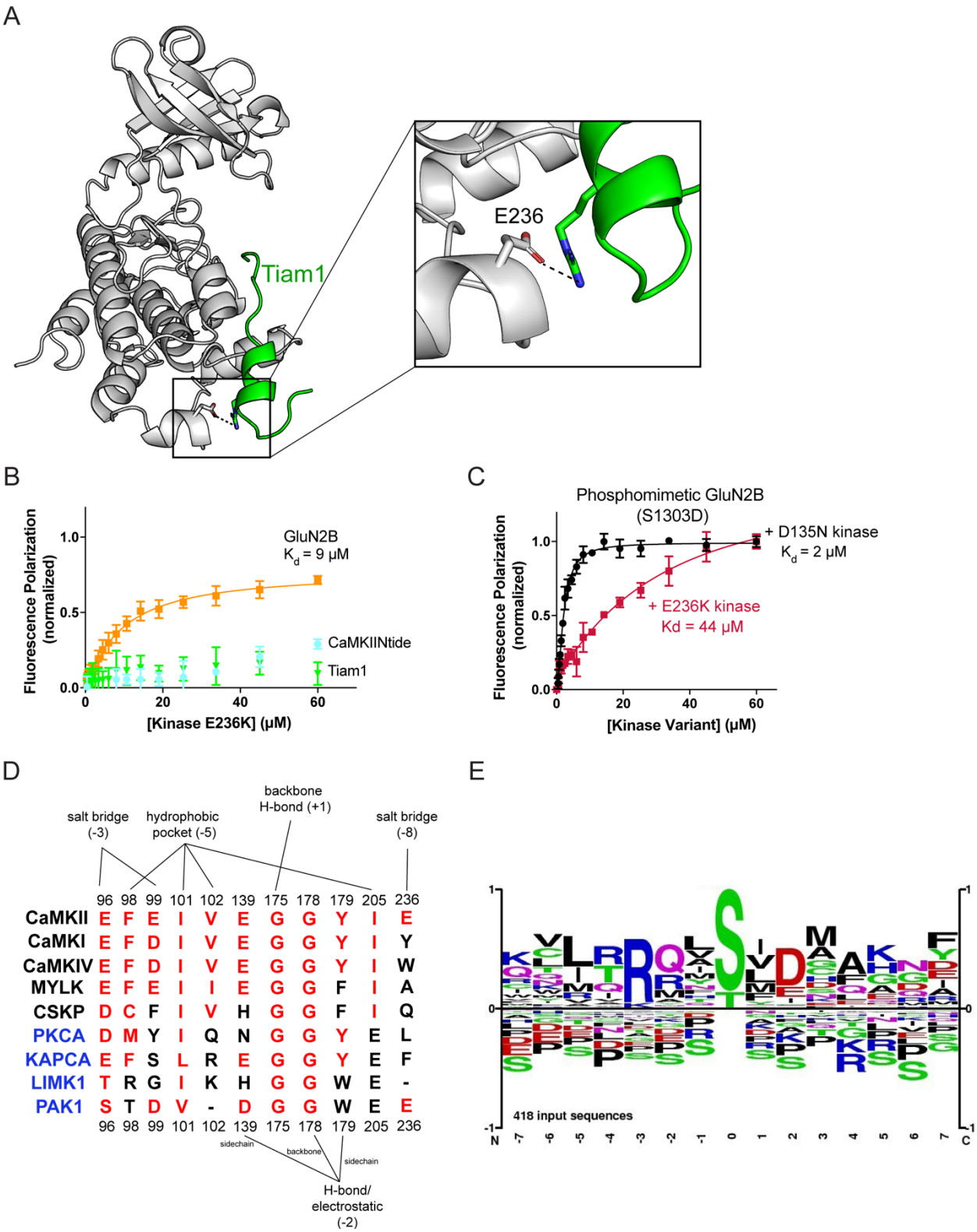

Figure 5. Electrostatic interaction with E236 has distinctive effects on binding. (A) View of the interaction between CaMKII E236 residue (gray) and Tiam1 R1549 residue (green). (B) FP measurements of the CaMKII kinase domain with E236K mutation binding to GluN2B (orange), CaMKIIN (cyan), and Tiam1 (green) peptides. (C) FP measurements of the phosphomimetic

GluN2B peptide (S1303D) binding to either WT CaMKII kinase domain (D135N, black) or mutant kinase domain (E236K, magenta). (D) Alignment of key residues involved in binding substrates across kinases from the Ca^{2+}/CaM family (black text) and four kinases from different families (blue text). PKCA and KAPCA (cAMP dependent kinase) belong to the AGC Ser/Thr family. LimK1 and Pak1 belong to TKL and STE Ser/Thr family. (E) The sequence logo for all previously identified substrates of CaMKII from the PhosphoSitePlus database with the phosphorylation site at the 0 position.

REFERENCES

1. Lisman, J., R. Yasuda, and S. Raghavachari, *Mechanisms of CaMKII action in long-term potentiation.* Nat Rev Neurosci, 2012. **13**(3): p. 169-82.
2. Malenka, R.C., et al., *An essential role for postsynaptic calmodulin and protein kinase activity in long-term potentiation.* Nature, 1989. **340**(6234): p. 554-7.
3. Sloutsky, R. and M.M. Stratton, *Functional implications of CaMKII alternative splicing.* Eur J Neurosci, 2020.
4. Erondu, N.E. and M.B. Kennedy, *Regional distribution of type II Ca2+/calmodulin-dependent protein kinase in rat brain.* J Neurosci, 1985. **5**(12): p. 3270-7.
5. Bayer, K.U., et al., *Interaction with the NMDA receptor locks CaMKII in an active conformation.* Nature, 2001. **411**(6839): p. 801-5.
6. Saneyoshi, T., et al., *Reciprocal Activation within a Kinase-Effector Complex Underlying Persistence of Structural LTP.* Neuron, 2019. **102**(6): p. 1199-1210 e6.
7. Bayer, K.U., et al., *Transition from reversible to persistent binding of CaMKII to postsynaptic sites and NR2B.* J Neurosci, 2006. **26**(4): p. 1164-74.
8. Walikonis, R.S., et al., *Densin-180 forms a ternary complex with the (alpha)-subunit of Ca2+/calmodulin-dependent protein kinase II and (alpha)-actinin.* J Neurosci, 2001. **21**(2): p. 423-33.
9. Jiao, Y., et al., *Characterization of a central Ca2+/calmodulin-dependent protein kinase IIalpha/beta binding domain in densin that selectively modulates glutamate receptor subunit phosphorylation.* J Biol Chem, 2011. **286**(28): p. 24806-18.
10. Diering, G.H. and R.L. Huganir, *The AMPA Receptor Code of Synaptic Plasticity.* Neuron, 2018. **100**(2): p. 314-329.
11. Barria, A., et al., *Regulatory phosphorylation of AMPA-type glutamate receptors by CaM-KII during long-term potentiation.* Science, 1997. **276**(5321): p. 2042-5.
12. Derkach, V., A. Barria, and T.R. Soderling, *Ca2+/calmodulin-kinase II enhances channel conductance of alpha-amino-3-hydroxy-5-methyl-4-isoxazolepropionate type glutamate receptors.* Proc Natl Acad Sci U S A, 1999. **96**(6): p. 3269-74.
13. Chao, L.H., et al., *Intersubunit capture of regulatory segments is a component of cooperative CaMKII activation.* Nat Struct Mol Biol, 2010. **17**(3): p. 264-72.
14. Castro-Rodrigues, A.F., et al., *The Interaction between the Drosophila EAG Potassium Channel and the Protein Kinase CaMKII Involves an Extensive Interface at the Active Site of the Kinase.* J Mol Biol, 2018. **430**(24): p. 5029-5049.
15. Wang, C., et al., *A novel endogenous human CaMKII inhibitory protein suppresses tumor growth by inducing cell cycle arrest via p27 stabilization.* J Biol Chem, 2008. **283**(17): p. 11565-74.
16. Zhang, J., et al., *Molecular cloning and characterization of a novel calcium/calmodulin-dependent protein kinase II inhibitor from human dendritic cells.* Biochem Biophys Res Commun, 2001. **285**(2): p. 229-34.
17. Chang, B.H., S. Mukherji, and T.R. Soderling, *Calcium/calmodulin-dependent protein kinase II inhibitor protein: localization of isoforms in rat brain.* Neuroscience, 2001. **102**(4): p. 767-77.

18. White, R.R., et al., *Definition of optimal substrate recognition motifs of Ca2+-calmodulin-dependent protein kinases IV and II reveals shared and distinctive features.* J Biol Chem, 1998. **273**(6): p. 3166-72.
19. Songyang, Z., et al., *A structural basis for substrate specificities of protein Ser/Thr kinases: primary sequence preference of casein kinases I and II, NIMA, phosphorylase kinase, calmodulin-dependent kinase II, CDK5, and Erk1.* Mol Cell Biol, 1996. **16**(11): p. 6486-93.
20. Ishida, A., et al., *Critical amino acid residues of AIP, a highly specific inhibitory peptide of calmodulin-dependent protein kinase II.* FEBS Lett, 1998. **427**(1): p. 115-8.
21. Stokoe, D., et al., *The substrate specificity and structure of mitogen-activated protein (MAP) kinase-activated protein kinase-2.* Biochem J, 1993. **296 (Pt 3)**: p. 843-9.
22. Coultrap, S.J. and K.U. Bayer, *Improving a natural CaMKII inhibitor by random and rational design.* PLoS One, 2011. **6**(10): p. e25245.
23. Yang, E. and H. Schulman, *Structural examination of autoregulation of multifunctional calcium/calmodulin-dependent protein kinase II.* J Biol Chem, 1999. **274**(37): p. 26199-208.
24. Rellos, P., et al., *Structure of the CaMKIIdelta/calmodulin complex reveals the molecular mechanism of CaMKII kinase activation.* PLoS Biol, 2010. **8**(7): p. e1000426.
25. Rust, H.L. and P.R. Thompson, *Kinase consensus sequences: a breeding ground for crosstalk.* ACS Chem Biol, 2011. **6**(9): p. 881-92.
26. Zha, M., et al., *Crystal structures of human CaMKIalpha reveal insights into the regulation mechanism of CaMKI.* PLoS One, 2012. **7**(9): p. e44828.
27. Mao, L.M., et al., *Phosphorylation and regulation of glutamate receptors by CaMKII.* Sheng Li Xue Bao, 2014. **66**(3): p. 365-72.
28. Kury, S., et al., *De Novo Mutations in Protein Kinase Genes CAMK2A and CAMK2B Cause Intellectual Disability.* Am J Hum Genet, 2017. **101**(5): p. 768-788.
29. Torres-Ocampo, A.P., et al., *Characterization of CaMKII alpha holoenzyme stability.* Protein Science, 2020.
30. McCoy, F., et al., *Metabolic activation of CaMKII by coenzyme A.* Mol Cell, 2013. **52**(3): p. 325-39.